

Global Design Of A Waveguide X-Band Power Amplifier

Alberto Leggieri, Davide Passi, Giovanni Saggio, and Franco Di Paolo

Dipartimento di Ingegneria Elettronica, Università degli Studi di Roma “Tor Vergata”

Via del Politecnico, 1-00133 Roma, Italy

alberto.leggieri@uniroma2.it. Website: <http://www.ehfrontier.uniroma2.it>

Abstract - The design and the fully coupled Thermodynamic and Structural Mechanics simulation of a Spatial Power Amplifier are described in this paper. The amplifier is realized in a WR90 waveguide, employing Fin-Line Transitions and Monolithic Microwave Integrated Circuit Solid State Power Amplifiers. Global performances of active devices and combining structure have a critical dependence to the thermo-mechanical condition of operation. The temperature alterations and thermal expansions, related to the power dissipation of the devices, have been analyzed in order to lead the amplifier at extreme power output, avoiding malfunctions. The proposed analysis accounts for the effects of different distributions of heat flux and stresses as a consequence of the different power consumption of the Driver and Final stage transistors. The amplifier combines 16 active devices of 7.9 W maximum power output with a power dissipation of 20 W, heating the transistor channel to 140° and deforming the mechanical structure to 4.9µm with a maximum stress of 0.41 GN/m². A maximum power output of 112W with a Return Loss greater than 12 dB in the whole X-Band is ensured.

Keywords: *Fin-Line structures, FEM simulations, Rectangular Waveguides, Power Amplifiers, Spatial Power Combiners, Heat Transfer, Structural Mechanics, and Multiphysics Simulations.*

I. INTRODUCTION

Spatial Power Amplifiers (SPA's) are a class of amplifiers which couple, in a parallel way, several single amplifiers in a defined space region. This general concept is shown in figure 1.

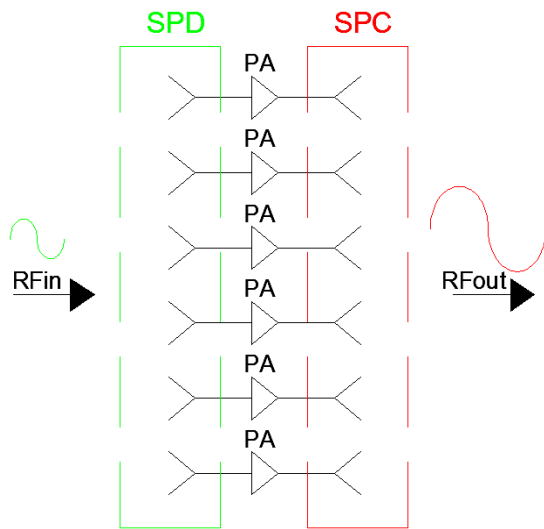


Fig. 1– The general concept of Spatial Power Amplifier.

A fundamental block of the SPA's is the Spatial Power Combiner (SPC), which is a passive reciprocal device that for this reason can also be called Spatial Power Divider (SPD): the SPC (or SPD) performs a parallel combining (or dividing) operation of many RF signals, thus reducing the combining (or dividing) loss to a minimum value. To realize an SPA, the RF signal entering a spatial region is captured by opportune EM

probes which divide the signal in a parallel way: this function realizes the SPD. Then, these signals feed SSPA's, and the amplified signals are summed in space through similar EM probes and, again, in a parallel way: this is done by the SPC.

SPA has an important role in fields of Power Amplifiers, especially in the High Frequency range. The classical approach to combine power signal is the binary combining [1-2]; it consists in a tree structure where the signals In_i whit $i=1...2N$, are added by binary combiners such as Wilkinson power combiners and reported in figure 2.

This solution is limited to the losses which each combiner inserts, and in addition limits the number of employed devices to a power of two.

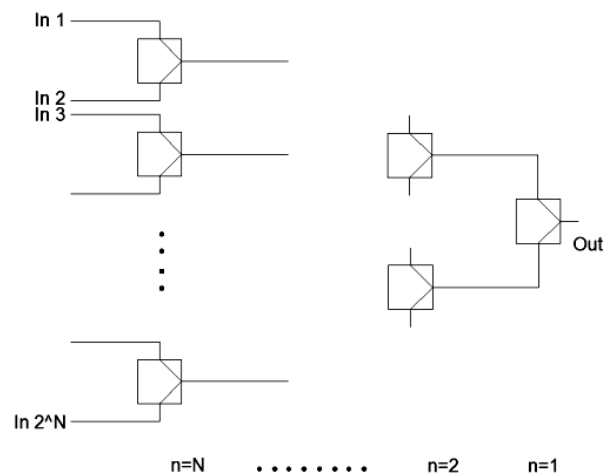


Fig. 2– The binary approach for a Power Combiner.

Conversely, spatial power combiners are based on signal power combination in low loss propagation inside the space of transmission lines [3], or even in open space [4]. When the signal combining and dividing is realized in a closed space several advantages result, as high device compactness, low combining losses and higher available power outputs.

A very important aspect to consider for any Monolithic Microwave Integrated Circuit (MMIC) Solid State Power Amplifiers (SSPA) design is that the power dissipation is unequally distributed in the MMIC volume. In fact, power is dissipated where the active devices are placed inside the MMIC; in addition, driver devices are typically of smaller size, and/or with a smaller number than the final devices. This determines a different path for the heat generated by the driver and for the heat generated by the final transistors. These energies, in the form of heat, combine and induce heat in several points of the material, and only with this driver-final dedicated analysis it is possible to determine if the transistor channels can be cooled.

This paper is organized as follows. In section II, the Waveguide SPA is described in detail. In section III the thermo-structural set-up needed for simulation is discussed. In section IV the simulation results are presented, and finally section V will summarize this work.

II. THE WAVEGUIDE SPATIAL POWER AMPLIFIER

A. General Considerations

The typical waveguide SPA configuration is based on rectangular WG and an array of Fin Line to microstrip transitions (FLuS's) printed on a dielectric substrate [3]. Many shapes of FLuS can be employed [5]; in this work we have used the exponential profile with antipodal configuration for the case of dual FLuS. This choice was driven according to [2]. As an example, in figure 3 the tapered cold and ground conductors on separate layers are shown for the case of a dual FLuS, while the substrate is not drawn. The whole assembly shown in figure 3 is simply abbreviated with the name "card".

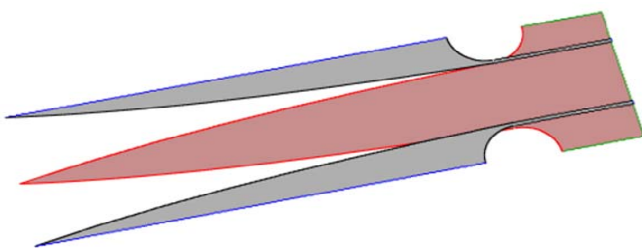


Fig. 3 – Double FLuS in antipodal configuration.

To improve the return loss, dielectric Quarter Wave Transformers (QWT) may be provided. This transformer helps the electromagnetic fields to adapt themselves to substrate load in the sense that no reflections occur, according to the small reflections theory [7].

The problem using the antipodal configuration is the difficult to obtain broadband response, since the transition creates a set of resonant modes which limit its useful bandwidth [6]. Near the terminal microstrip section of

antipodal FLuS transition, where quasi TEM mode are being generated, TE_{10} mode tends to cutoff, and evanescent modes are being created, storing inductive energy. The Fin-Line discontinuity appears to the evanescent modes as a parasitic slot in a bisecting metal sheet. In this region electric field will be created, storing capacitive energy. When the capacitive energy created by the slot equals the inductive energy stored in the evanescent modes, a resonance will occur [6]. In order to avoid this resonance, the Fin-Line discontinuities can be designed so as to break the slot electric field lines. An useful solution has been applied; it consists to model a circular section through the metal sheet in the area where the parasitic slot might create [6].

The power traveling in the input WG section is captured by FLuS's, and carried by microstrip transmission lines to MMIC SSPA's. The outgoing power from the amplifiers is sent to other FLuS's, which combine the amplified RF signal to the WG output section. More than one FLuS can be printed on a card, allowing the use of more MMIC's on the same card. In this design, we have used a card with Quad FLuS's [9] as shown in figure 4, with a wireframe view for a better understanding: a parallel QWT at the beginning of the card is evident [9].

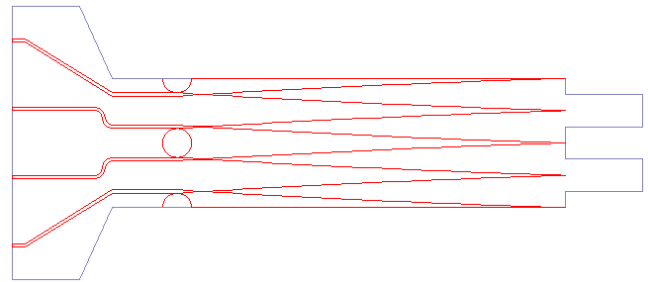


Fig. 4 – A card with four antipodal FLuS's and a p-QWT.

In general, oversized waveguides are used in those applications where MMIC's sizes are greater than the available space inside the waveguide. To verify this, let us consider the very used waveguide type WR28, for Ka-Band operation. A PA MMIC operating in a part of such band is for example the type TGA4916 produced by Triquint, whose dimensions in mm are $a_m=3.86 \times b_m=5.71 \times t=0.05$, with the RF input and output pads placed at the side of the MMIC widest dimension b_m . Comparing this value of b_m with $b=3.556$ mm of the WR28 waveguide, it results no available space inside the WR28 waveguide to insert such MMIC.

However, a very careful design is needed for oversized structures enclosing amplifiers, to avoid the growth of unwanted spurious amplified bands and/or oscillations. While tapering in waveguide width can be considered relatively simple, at least when the cut-off frequency of the TE_{30} has not overcome, for the tapering in height must be paid more attention. In fact, in addition to TE high order modes, the creation of a z-component of the electric field in a height taper can introduce parasitic TM modes. If the height $b=10.16$ mm of a standard WR90 waveguide is increased to 32mm it is possible that TE_{12} mode couples to TM_{12} mode.

A common solution to the problem of the available space for MMIC's inside the waveguide, not recurring to an oversized waveguide, is to transform the waveguide mode to a 2 wire transmission line mode, like the q-TEM mode of the microstrip, as we propose for the FLuS's shown in figure 3 and 4. After transforming the waveguide mode into microstrip mode, it is possible to enlarge the waveguide so to insert the MMIC's, reducing the problems otherwise occurring with oversized waveguide where multiple modes are excited. This is a successfully adopted and general solution [8-9], and applied in our study too as later reported.

B. The Fin Taper Profile

In order to reduce the combining loss, the shape of the FLuS taper requires a shape useful to minimize the return loss within the frequency band of interest.

Several spatial profiles of FL can be implemented: exponential, parabolic, sine, sine squared, cosine and cosine squared taper [5]. We selected the former with the aims to ensure the smoothness of the taper and to reduce the reflection for the incident power. The spatial profile of an exponential Fin taper is given by:

$$w(z) = w_0 \exp\left[\frac{z}{l} \ln(w_f)\right] \quad (1)$$

where w_0 and w_f stands respectively for initial and final taper width, while l is the total length of the transition [5].

The position dependent impedance of an exponential Fin taper is given by [5]:

$$Z(z) = Z_0 \exp\left[\frac{z}{l} \ln \frac{Z_1}{Z_2}\right] \quad (2)$$

where Z_2 is the impedance to match, that is the waveguide port impedance, Z_1 is the matching impedance, generally 50Ω , and z is the coordinate of the longitudinal axis.

By employing the small reflections theory [7], the spatial profile $w(z)$ has been taken as the uniform TL characteristic impedance $Z(z)$. From Riccati's equation it is possible to find the reflection coefficient trend [10] with respect the product βl that is given by:

$$\Gamma = \frac{1}{2} e^{-j\beta l} \ln\left[\frac{Z_1}{Z_2}\right] \frac{\sin(\beta l)}{\beta l} \quad (3)$$

Microstrip Lines have been designed following Hammerstad formulas reported in [11]. By means of in house realized software routines, developed according to the Pramanick and Bhartia procedure [5], we evaluated around 290Ω waveguide port impedance. A typical output of our routines is reported in Figure 5 for the taper impedance vs. taper width.

The Quad FLuS tapers employed in the proposed SPA have been evaluated accordingly with the before mentioned theory and software.

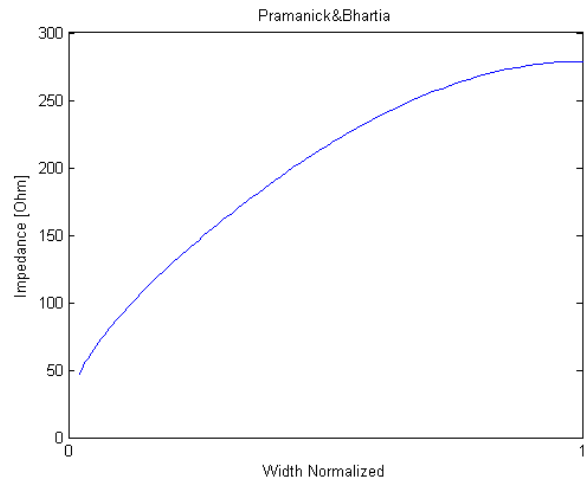


Fig.5-Taper impedance vs. taper width computed by the custom software.

C. The Analyzed SPA

Fitting with our purposes, we considered to analyze the structure of an SPA operating in X-Band, employing TGA9083 MMIC's produced by Triquint [12], a commercial device with a good price to value ratio. This SPA is realized in a WR90 waveguide, with a central part made of three metal carriers holding antipodal FLuS's and MMIC SSPA's. The material to be use for the carrier has been investigated in this work, looking for the best compromise in term of heat transfer and mechanical stress.

One carrier is placed at the center of the waveguide, while the other two are symmetrically placed from the center. The center carrier holds, for each face, 2 FLuS's printed on Alumina substrate and 4 MMIC's; each lateral carrier holds 4 MMIC PA's and two FLuS's. This SPA is shown in figure 6.

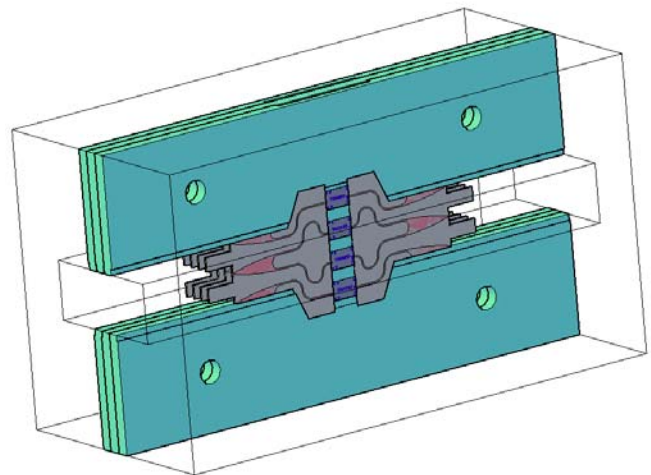


Fig.6-Three carries, 16 MMIC's, inserted in a WR90 waveguide.

It is worth noting that the needed area to place the used MMIC's, also considering associated filtering capacitors, is greater than what available in the WR90. However, since microstrip propagation modes are available after the FLuS, we have taken the needed transversal place for the MMIC's at this position without affecting waveguide propagation mode.

Each card is 30mm length and has four 50Ω microstrip lines (0.25mm width) printed on to bring to MMIC amplifiers the EM power. In adding a 6mm p-QWT has been employed to get the best return loss.

This structure is doubly symmetric respect two longitudinal orthogonal planes, a noteworthy property that considerably helps in reducing the complexity of the simulation. This is because only one quarter of the complete structure (reported in figure 7) has to be simulated, so reducing the required number of meshes.

The power dissipation of the MMIC SSPA's produces a considerable temperature increase and induces a thermal expansion of both the PA's and the connected structure. If the SSPA's temperature exceeds the maximum allowed value (specified by the SSPA's manufacturer), an amplification failure or device damage may occur.

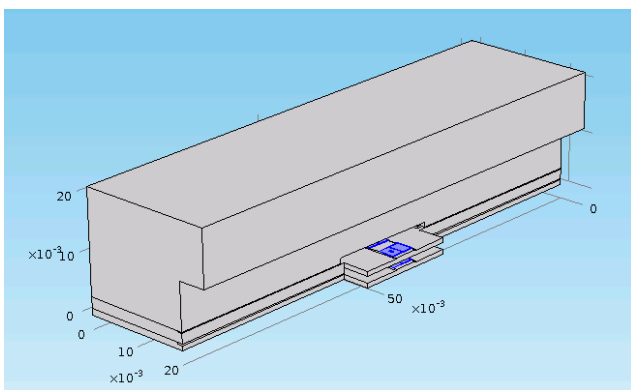


Fig. 7-One quarter of the SPC in WR90 waveguide, ready to simulate.

The thermal expansion of the materials may also induce significant stresses and strains, with a consequent displacement of the guiding and combining structures, which alter the desired Electromagnetic (EM) behavior of the SPC.

Many MMIC SSPA's are composed by a driver stage and a final stage FET's, but quite often Thermodynamic analysis are performed considering the amplifiers as a unique heat sources, which dissipate the total power in all their volumes [3,8,13] or sometimes this important analysis is not even performed [14].

The problem of this Thermodynamic approach is that it doesn't allow understanding if a determined area of the integrated circuit exceeds the maximum rated temperature, as the channel temperature. Driver devices are smaller than the final, and have a typical power dissipation which is generally estimated, when the exact values are not available, as the total power dissipation multiplied for the ratio of the driver volume and the final volume: the remaining one is dissipated by the final stage. The difference of heat power distributions between the two active stages determines a different path of the heat generated by the driver and the heat generated by the final transistor. These energies, in the form of heat, combine and induce heat in several points of the material, and only with this driver-final dedicated analysis is possible to determine if the transistor channels can be cooled.

The specific heat flux paths determine specific thermal expansion of the materials in different portions of the SSPA volume, which induce specific compressive forces distribute

in the subjected areas. Stresses and strains are thus applied to the device, and need to be computed.

The thermal expansion of the materials may also induce significant stresses and strains with consequent displacement of the guiding and combining structures, which alter the desired Electromagnetic (EM) behavior of the structure. We analyzed the Thermodynamic effects induced by the power dissipation in the driver and final stage of the TGA9083, instead to consider the dissipated power equally distributed in the MMIC volume.

III. THERMO-STRUCTURAL MODEL SET-UP

A Thermodynamic stationary analysis allows the computation of the temperature when the heat generated has been diffused on all the reachable SPA components. In this condition, the system has become thermally stable, giving a fixed temperature over all the SPA outer boundaries. A Structural Mechanics stationary analysis can be employed to estimate the deformation induced by the thermal expansion of the material induced by the heat generated by the SSPA's power dissipation.

A Finite Element Method (FEM) based simulation using COMSOL has been employed to couple Thermodynamic and Structural analysis by storing thermodynamics information. In order to decrease computational time and resources maintaining accuracy, the device model has been organized by using several computational strategies.

In order to compute the temperature and the thermal expansion of the SPC, the model has been organized by using Heat Transfer in Solids (HT) and Solid Mechanics (SM) COMSOL modules [15]. Since it has been assumed that the temperatures are independent with respect to the displacements, a separate computation has been adopted, for the temperature using the HT module and for the displacement using the SM module.

The mechanical boundary conditions have been chosen in order to leave the WG external walls free from any constriction, ensuring the boundaries ability to swell. This condition avoids any normal force on the WG walls and any rotation, allowing computing the complete deformation of the SSPA's induced by the thermal expansion of the materials.

By using the default normal settings of COMSOL mesh interface, an accurate discretization has been reached with moderate computational cost. The study has considered the adoption of two separated steps: the first stationary step has been employed to calculate the temperature distribution, through the HT module, and the second stationary step to solve for the displacements, through the SM module.

In order to consider the results of the HT analysis, the information on the computed temperature distribution has been inserted as the temperature in the Thermal Expansion sub-node of the Linear Elastic Material feature in the SM module. By means of the SM module the meshes have been moved in function of the displacement computed by the Thermal Expansion analysis.

Heat Transfer has been computed by solving the Heat Equation in the steady state [15]:

$$-\nabla \cdot (k\nabla T) = Q \quad (4)$$

where T is the temperature, k the thermal conductivity of the material and Q is the heat power density.

The solid model is intended as isotropic and the structural transient behavior as quasi-static. The stationary analysis consists in solving the [15]:

$$-\nabla \cdot \sigma = \bar{F}_V \quad (5)$$

Where σ is the stress and \bar{F}_V is the force per unit volume.

IV. ELECTROMAGNETIC MODEL SET-UP

A 4 cards rectangular WG-based X-band SPC has been designed, in which exponential tapered FL transitions are mounted on the previous analyzed cards, placed inside the WG. The FLuS are made on Al_2O_3 substrate, with a thickness of 0.254 mm. Each card contains two FLuS connected back to back with double symmetrical QWT sections. These cards are supported by three carriers. Carrier volumes are not inserted in the electromagnetic model but their surfaces are represented with a particular boundary condition which allows the surface losses computation.

The electromagnetic model of the proposed structure has been simulated by using HFSS version 15 of Ansys-Ansoft.

A stationary analysis has been employed to solve the wave equation in the frequency domain (6) [15].

$$\nabla \times \mu_r^{-1} (\nabla \times \bar{E}) - k_0^2 (\epsilon_r - \frac{j\sigma}{\omega\epsilon_0}) \bar{E} = 0 \quad (6)$$

Where μ_r is the magnetic permeability, ϵ_r the electrical permittivity and σ the electrical conductivity of the material; ϵ_0 is the electrical permittivity of the vacuum, k_0 the wave number in free space, ω the wave angular frequency and \bar{E} the electric field. We selected the copper as FLuS conductors, stand its excellent thermal conductivity. Since a good discretization of the Fin taper profile was of fundamental importance, the exponential profile was approximated with a discrete number of points such that the different segment obtained were smaller than $\lambda/20$ at the highest frequency of the operative band. In this way the discretization doesn't affect the performance but reduces the computational complexity.

V. COMPUTATIONAL OUTPUTS

A. Temperature

We have imposed a power dissipation of 20 W for each of the 16 MMIC's, considering the conversion efficiency of the used MMIC's. The temperature has been computed at the channels of the MMIC's when the carrier is realized with aluminum. Figure 8 shows the temperature in the channel of the final stage to be around 250 °C, well above the maximum MMIC allowed temperature. So, we have repeated the Thermodynamic simulation when using Copper carriers and the results are given in figure 9. In this case, the channel temperature reaches a maximum of 140°C, which is below the

maximum allowed temperature.

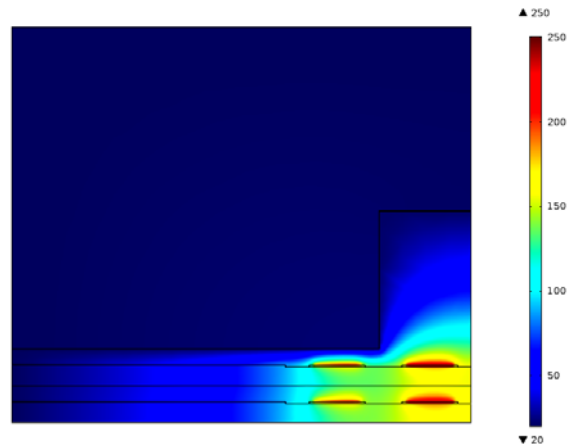


Fig.8-Temperature [°C], with Aluminum carriers.

It is important to show that the assumption of an uniform power dissipation throughout the MMIC will results in a highly underestimated temperature. In fact, figure 10 demonstrates the resulting temperature when MMIC power dissipation is assigned to the whole MMIC volume that is an uniform power distribution.

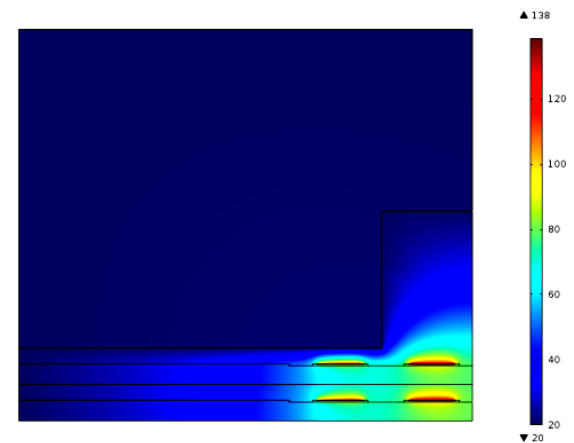


Fig.9-Temperature [°C], with Copper carriers.

A maximum temperature of 81.5°C is estimated, as reported in figure 10, well below the 140°C simulated in the channel when power dissipation is concentrated in the active device channels.

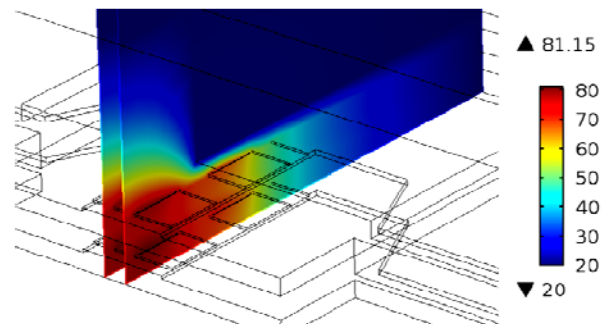


Fig.10-Temperature [°C], with Copper carriers and uniform power distribution: zoom view.

B. Stress and Displacement

By receiving the Temperature computation from the HT analysis, the SM study allows to evaluate the stress and strain in any part of the structure. Copper carriers are used. In figure 11 the maximum stress results to be located near the oblique angles of the cards and locally reaches 0.41 GN/m^2 .

The maximum displacement is near the interface between the innermost SSPA's and the slab copper support, which is of $4.9 \mu\text{m}$, negligible from the RF guiding properties of the structure (figure 12).

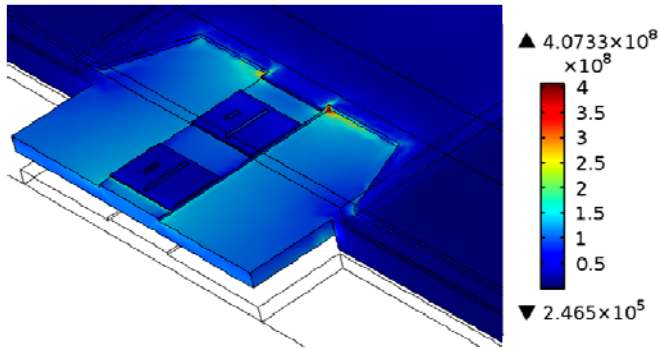


Fig.11- The stress inside the structure [Nm^{-2}].

This is an appreciable result, since this displacement value is completely incompatible with the GaAs survivability to displacement. For such a reason, an interface layer is needed between the back of the GaAs MMIC and the copper carrier, adopting CuW or CuMo as materials. Moreover, by employing this Thermo-mechanical design, the appropriate heat-sinker profile has been chosen so that the MMIC amplifiers can be driven at full power.

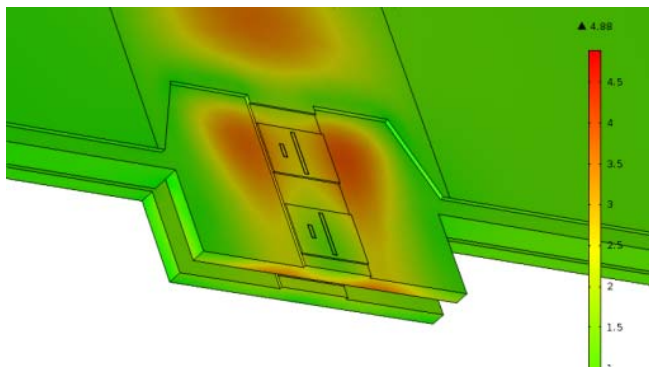


Fig.12- The displacement is inside the structure [μm].

C. Scattering parameters and Power Output

The reflection and transmission S-parameters versus frequency have been computed. The results are plotted in figures 13 and 14 respectively.

Since the MMIC devices are brazed on cards placed near the center of the WG on different positions, a couple of cards receive a certain portion of power different to the other couple. In particular, from figure 14 we note that nearly 1.5dB of different illumination exists between the couple consisting of the two central with the couple formed by the two external

cards. In the whole X-Band, we have a minimum Return Loss of 12dB. The maximum simulated Insertion Loss of the passive structure is less than 1dB, as shown in figure 15. By taking into account such losses, and since each TGA9083 can reach a maximum power of 39dBm [12], the proposed Spatial Combining Amplifier can reach a maximum output power of 50.5dBm with about 89% of combining efficiency.

This result has been obtained considering some idealities that are MMICs perfectly matched with no phase distortion and linear gain.

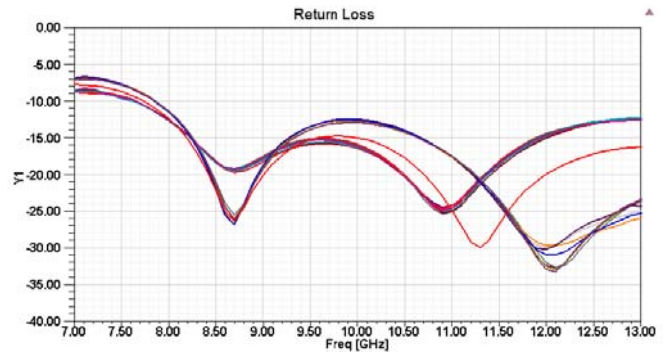


Fig.13-The simulated reflection scattering parameters.

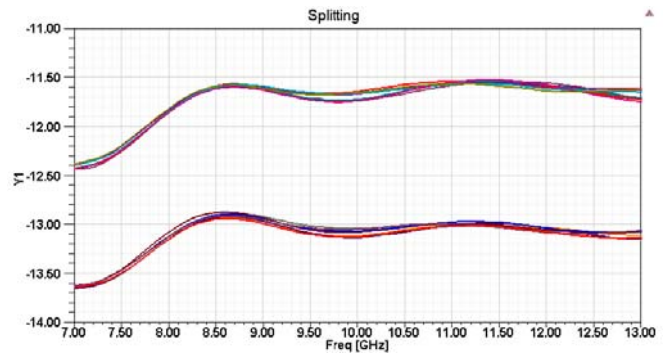


Fig.14-The simulated transmission scattering parameters.



Fig.15-The simulated insertion loss of the passive SPC.

VI. CONCLUSIONS

A global multiphysics study is proposed for the design of a Spatial Power Combining Amplifier operating in the whole X-band. This technology has been studied using Finite Element Method employing commercial software where Heat Transfer,

Structural Mechanics and Electromagnetic simulations are performed. Temperature distributions and related structural conditions, such as stress and displacement, are been computed, together with the EM behavior of the device.

The proposed analysis accounts for the effects of different distributions of heat flux and stresses as a consequence of the different power consumption of the Driver and Final stage transistors. The amplifier combines 16 active devices of 7.9 W maximum power output with a power dissipation of 20 W, heating the transistor channel to 140° and deforming the mechanical structure to 4.9µm with a maximum stress of 0.41 GN/m²

The in-frequency electromagnetic behavior of the proposed structure has been investigated by computing S-parameters. This analysis allows the proper thermodynamic and structural design for such amplifiers, so that proper materials for carriers and device interfaces can be selected. The proposed device can provide a maximum power output of 112W with a Return Loss greater than 12 dB in the whole X-Band and a size of 40x40x100 (units mm).

REFERENCES

- [1] K.J.Russel: "Microwave Power Combining Techniques", IEEE Trans. on MTT Vol. MTT-27, N. 5, May 1979, pp.472-478.
- [2] K. Chang, C. Sun: "Millimeter-Wave Power Combining Techniques", IEEE Trans. on MTT Vol. MTT-31, N. 2, Feb 1983, pp.91-107.
- [3] A. Leggieri, G. Orengo, D. Passi, and F. Di Paolo: "The Squarax Spatial Power Amplifier", PIER-C, Vol. 45, 2013, pp.43-45.
- [4] J. Harvey, E.R. Brown, D.B. Rutledge, R.A. York: "Spatial Power Combining for High Power Transmitters", IEEE Microwave Magazine, Dec. 2000, pp.48-59.
- [5] B. Bhat, S.K. Koul: "Analysis, Design and Optimization of Fin Lines", Artech House, 1987.
- [6] George E. Ponchak, Alan N. Downey: "A New Model for Broadband Waveguide to Microstrip Transition Design", NASA Technical Memorandum 88905, Lewis Research Center Cleveland, Ohio, December 1986.
- [7] R.E.Collin: "Foundations for Microwave Engineering", McGraw Hill Series in Electrical and Computer Engineering, II Ed., 1992.
- [8] D.An, X.K. Li, J.C. Mou, X. Liv: "A new type of Ka-band waveguide-based power-combining structures", Intern. Conf. on Microwave and Millimeter Wave Tech., 2008, Vol: 1, pp.347-350.
- [9] D.Passi, A.Leggieri, F. Di Paolo, M. Bartocci, A. Tafuto, A. Manna: "High Efficiency Ka-band Spatial Combiner", Advanced Electromagnetics, Vol 3, No 2 (2014), pp. 10-15.
- [10] D. M. Pozar: "Microwave Engineering", John Wiley & Sons, 1998, ISBN 0-471-44878-8.
- [11] F. Di Paolo: "Networks and Devices Using Planar Transmission Lines", CRC Press LLC, 2000, ISBN 0-8493-1835-1.
- [12] TriQuint Semiconductor: "TGA9083-SCC, 6.5-11.5 GHz High Power Amplifier", Product Data Sheet, TriQuint Semiconductor.
- [13] Nai-Shuo Cheng, Pengcheng Jia, David B. Rensch, and Robert A. York: "A 120-W -Band Spatially Combined Solid-State Amplifier", IEEE Transactions on Microwave Theory and Techniques, Vol. 47, N. 12, December 1999, pp. 2557-2561.
- [14] Y. Ning, J. Sun, J. Liu, W. Jiang: "A new spatial power combiner based on 32-way ridged waveguides", General Assembly and Scientific Symposium, Beijing, 16-23 Aug. 2014, pp. 1-4.
- [15] A. Leggieri, D. Passi, F. Di Paolo: "Multiphysics Modeling Based Design of a Key-Holes Magnetron" Proc. of IEEE International Conference on Numerical Electromagnetic Modeling and Optimization, Pavia, Italia, 2014, pp.1-4.

AUTHORS

Alberto Leggieri received his Degree in Electronic Engineering in 2011 from University of Rome "Tor Vergata". Now, he is with S.I.T. S.p.A as R&D Engineer and R.F. Laboratory Manager in developing IORT dedicated electron accelerators, and he is attending the Ph.D. course in Electronic Engineering in developing High Power Microwave devices such as Power Spatial Combiners, Vacuum Tubes and Passive Structures. He upgraded the accelerating structures and designed several Electromagnetic and RF-MW devices of the mobile e-IORT accelerators LIAC and LIAC-S. His research interests are in applied electromagnetism, MMIC devices, Vacuum Tubes, LINACs, and Multiphysics Modeling. alberto.leggieri@uniroma2.it



Davide Passi received his Master's Degree in Electronic Engineering in 2013, from University of Roma "Tor Vergata". Now he is attending the Ph.D. course in Electronic Engineering. His research interests are in Applied Electromagnetism, MMIC devices, Solid State microwave Power Amplifier and Spatial Power Combining Techniques. davide.passi@uniroma2.it



Giovanni Saggio received the degree in Electronics Engineering in 1991 and the Ph.D. in Microelectronics and Telecommunication Engineering in 1997, both at the University of Rome "Tor Vergata". He won one Fellowship by Texas Instruments and two Fellowships by the Italian National Research Council (CNR). He has spent several years in University as Glasgow, Cambridge and Oxford. He has been project leader of researches for the Italian Space Agency (ASI), for the Avionic Service of the Italian Defence Department (Armaereo), for the Italian Workers' Compensation Authority (INAIL). Now he is with the University of Rome "Tor Vergata" (Italy). His research interests are in Electronic noise, SAWs, Electronic sensors and, more recently, Biotechnology. He is currently member of the Italian Space Biomedicine, founder and manager of HITEG (Health Involved Technical Engineering Group). Email: saggio@uniroma2.it



Franco Di Paolo received his Laurea Degree in Electronic Engineering in 1984 from University of Roma "La Sapienza". He has spent several years as microwave circuit designer in industries as Fatme-Ericsson S.p.A, Elettronica S.p.A, Telit S.p.A, Finmek-Space S.p.A. Now, he is with the University of Roma "Tor Vergata", Italy. His research interests are in Applied Electromagnetism, Solid State microwave Power Amplifier, Vacuum Tube microwave Power Amplifiers. He is an IEEE Associate Member of MTT Society. Email: franco.di.paolo@uniroma2.it

